Harvesting red fluorescence through design specific tuning of ICT and ESIPT: an efficient optical detection of cysteine and live cell imaging†

Uzra Diwan,[a] Virendra Kumar,[a] Rakesh K. Mishra,[b] Nishant Kumar Rana,[c] Biplob Koch[c] and K. K. Upadhyay*[a]

In this report, we constructed 2-(2-hydroxyphenyl)benzothiazole (HBT) based ratiometric fluorescent probe R1, highly selective for cysteine (Cys) in the red channel with a nanomolar detection limit. The rational combination of benzothiazole and benzothiazolium unit within the same molecular frame work act as "two-heads" that allowed the simultaneous harvesting of intramolecular charge transfer (ICT) as well as excited state intramolecular proton transfer (ESIPT). This coupling of dual mechanism in R1 provides selective colorimetric and ratiometric fluorescence response towards Cys from the mixture of various anions and amino acids including foremost interfering thiols *viz.* HS⁻, Hcy and GSH. R1 shows a weak ESIPT at 497 nm (green fluorescence, N*) which undergoes shifting to 625 nm (red channel K*) upon addition of Cys selectively. Henceforth, R1 was also utilized for marking Cys in live cell imaging in HeLa cells. The sensing phenomenon of R1 for Cys was studied through a number of spectroscopic techniques *viz.*, NMR, IR along with HRMS studies. The density functional theory calculations further strengthened the experimental findings.

Introduction

The ingenious design and development of small molecular probes for selective *in situ* monitoring of bio-thiols *viz.*, cysteine (Cys), homocysteine (Hcy) and glutathione (GSH) is highly desirable and has been an attractive area of research since the last few years.[1–5] The selective recognition of cysteine is quite important, as it is known to play crucial role in several biological activities of proteins, oligopeptides and enzymes *etc.*[6–8] Additionally cysteine also protects the neurons from various diseases like Alzheimer's, Parkinson's as well as helps to convert several toxic heavy metal compounds into stable complexes which can be easily discharged from the body.[9–11] The optical detection methods involving chemosensors have been proven better than instrumental methods which are normally used in routine.[12–16] The ratiometric fluorescence detection adds up the quality to the optical probes by increasing the dynamic range of measurement which finally leads sensitivity and precision to the measurements.[17–19] The ratiometric probes reported

hitherto for the detection of the thiol containing amino acids (Cys, Hcy) and tripeptide (GSH) are either based on the simple ICT probe, ESIPT probe or on chemodosimetric approach. The addition of analytes to these probes causes well separated fluorescence emission peak by modulating/interrupting the π-conjugation, the electron cloud or by releasing the fluorophore.[20–24] Amongst these the excited state intramolecular proton transfer (ESIPT) that occurs in H-bonded conjugated ring accompanied by photoinduced tautomerization usually exhibits large stokes shift as well as dual emission band characteristics of keto-enol form.[25–27] The ESIPT probes commonly employ derivatives of 2-(2-hydroxyphenyl)benzoxazole (HBO),[28] 2-(2-hydroxyphenyl)benzothiazole (HBT)[29] and 2-(2-hydroxyphenyl)benzimidazole[30] *etc.* These probes have got numerous applications from the view point of sensing of a number of analytes *viz.*, Pd^{2+}, Hg^{2+}, Zn^{2+}, H_2S, HSO_3^- *etc.*[31–33] The same are also relevant with respect to photo-switches and organic LEDs *etc.*[34]

Taking into account the appealing features of ESIPT dyes and biological importance of Cys, the HBT derived sensor for Cys till date, have been shown in Scheme 1.

The sensing approach in these sensors can be divided into two types; type-a: one with the nucleophilic attack of biothiols on the aldehyde[35] and type-b: the regeneration of the free hydroxy group (chemodosimetric approach) which is generally protected by bromoacetyl or bromopropionyl groups.[36,37]

The coupling of ESIPT along with ICT in the fluorescent probes hitherto induced small stokes shifts and lead fluorescence

[a]Department of Chemistry (Centre of Advanced Study), Institute of Science, Banaras Hindu University, Varanasi-221005, India. E-mail: drkaushalbhu@yahoo.co.in

[b]Photosciences and Photonics Section, Chemical Sciences and Technology Division, CSIR – National Institute for Interdisciplinary Science and Technology, Thiruvananthapuram-695019, India

[c]Department of Zoology (Centre of Advanced Study), Institute of Science, Banaras Hindu University, Varanasi-221005, India
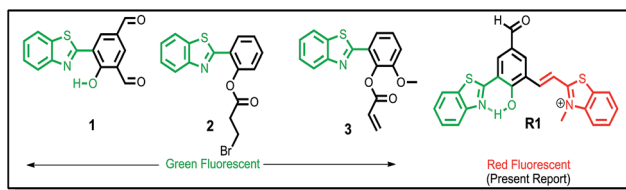
Scheme 1 Some of the previous and present approaches utilized for fluorescent detection of Cys through HBT based sensors.
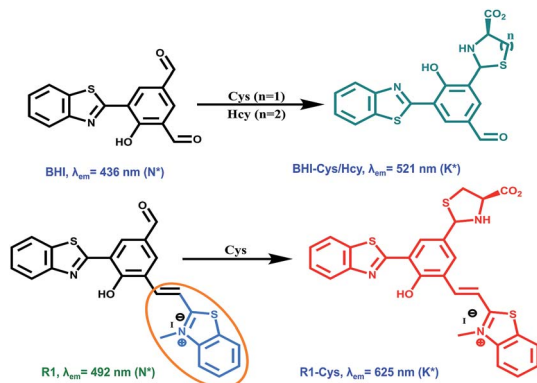
Scheme 2 Design strategy and fluorescence response of BHI (already reported probe) and probe **R1** (present study).

in the blue to green channel only. Recently, Yang *et al.* has also reported a rohodol thioester based sensor for biothiols with distinct fluorescence emissions by the combination of as photo-induced electron transfer (PET) and ESIPT mechanism.[38] Frequently, these measurements suffered considerable interferences from Hcy/GSH with optimum detection limit and time response (Table S1†).

Concerning the aforementioned concepts, we report herein an HBT based ratiometric probe **R1** for cysteine in aqueous medium in the red channel with high sensitivity and selectivity over other similar type of biothiols such as Hcy and GSH. The designing of the probe **R1** involves condensation of one of the aldehyde group of its precursor compound BHI (an already reported ESIPT based sensor for Cys/Hyc)[35] with benzothiazolium iodide. The presence of both, benzothiazole and benzothiazolium iodide group within the same molecular framework **R1**, lead judicious combination of ICT with ESIPT (Scheme 2). The same causes large stokes shift and allows ratiometric sensing of Cys selectively in the red channel with nanomolar detection limit along with fast response time.

Results and discussion

Design and synthesis of probe R1

As mentioned above, HBT derived moieties are well known fluorophore that exhibits excellent ESIPT phenomenon, often with dual emission which particularly lie in the blue and green channel.[39] Despite of its superior candidature as a fluorescent sensor, usually the need of high excitation energy limits the biological applicability of these HBT dyes. On the other hand, the fluorescence in the red region which provides low auto-

fluorescence and can penetrate deeper inside the living tissues are found to be more bio-compatible over conventional blue and green emitting probes.[40,41]

The rational design of the probe **R1** was in order to bestow; (i) excited state intramolecular proton transfer (ESIPT) behavior *via* HBT, (ii) longer wavelength emission in the red channel, by incorporating benzothiazolium unit and (iii) an electrophilic site for the selective attack of Cys *i.e.* free aldehyde group (Scheme 3).

Photo physical properties of probe R1

As it is well known that the ICT and ESIPT probes are sensible to the environment, hence we studied the effect of different solvents of varying polarity on the probe **R1** (Fig. S1, ESI†). The absorption maximum in non-polar solvent such as $CHCl_3$ appeared at 590 nm, was assigned to the intramolecular charge transfer (ICT) band. However, a noticeable blue shift was observed in the same as we move from non-polar to polar solvent (Fig. 1a), highlighting the negative solvatochromism which may be due to unlike extents of stabilization of ground and excited states.[42] The probe **R1** is expected to exist in two tautomeric forms *viz.*, enol and keto forms and the same was reflected in the form of dual emission bands at 470 nm and 680 nm in $CHCl_3$ (Fig. 1b). The small band at 470 nm was observed as well defined emission band of normal enol form in the excited state (E*) while the emission maximum 680 nm was assigned to the excited keto (K*) form. It was noted that increase in solvent polarity shifts the equilibrium towards the enolic form which further lead to decrease in the ratio of keto/enol form. This finding was in well accordance with the literature, where the ESIPT got quenched due to the presence of inter-molecular H-bonding in polar solvent.[43–45]

Optical sensing studies

The sensing ability of **R1** (10 μM) towards specific analyte was performed in a mixture of $H_2O : ACN$ (7 : 3, v/v). The **R1** was
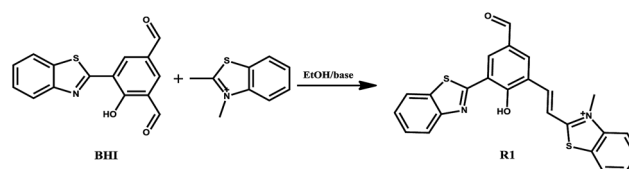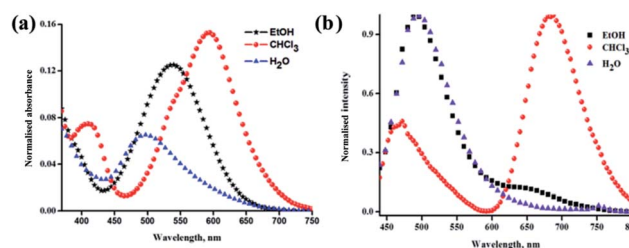

Scheme 3 Synthesis of probe **R1**.

Fig. 1 Effect of solvent polarity on absorption (a) and fluorescence (b) spectra of **R1** (λ_{ex} = 430 nm).

pink in color and displayed an absorption maximum at 502 nm along with a broad band ranging from 355–305 nm. When we gradually added (1–10 equivalents) Cys to the **R1** its color got bleached (Fig. S2, ESI†). The ICT band showed depletion tendency while a new band at 397 nm was gradually evolved. As shown in Fig. 2, the titration profile of **R1** in the presence of Cys showed two well-defined isosbestic points at 430 nm and 373 nm, emphasizing the conversion of **R1** to a new species. The lowest detection limit from above titration profile was estimated to be 1.21×10^{-6} M in the linearity range of 5.0×10^{-6} to 6.0×10^{-5} M (Fig. S3, ESI†) and the data got fitted in 1 : 1 binding equation yielding association constant value of $(5.21 \pm 0.90) \times 10^{4}$ M^{-1} ($R^2 = 0.993$) (Fig. S4, ESI†).

In the emission spectrum, we observed a ratiometric fluorescence change from green to red in the presence of Cys upon exciting **R1** at 430 nm (Fig. S5, ESI†). The fluorescence titration study with the sequential addition of Cys from 0.1 to 20 equivalents showed a decreasing trend in the enolic peak (492 nm)
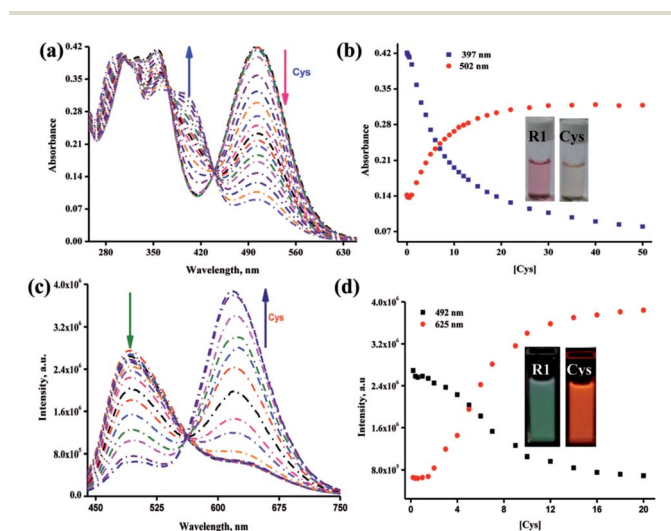
with a consecutive increase in keto (625 nm) emission (Fig. 2). The binding constant was calculated on the basis of nonlinear fitting using the above titration studies. The data got, excellently fitted in 1 : 1 binding equation (Fig. S6, ESI†) with the binding constant value of $(7.50 \pm 1.20) \times 10^{5}$ M^{-1} ($R^2 = 0.995$) and the lowest detection limit was found to be 4.61×10^{-8} M with a linearity range of 7.50×10^{-6} to 4.50×10^{-5} M (Fig. S7, ESI†).

Selectivity studies

As selectivity is one of the major requirements for the quantification of an analyte. Hence we tried to quantify the selectivity of probe **R1** *via* UV-vis as well as fluorescence emission studies towards various anions *viz.*, F$^-$, Cl$^-$, Br$^-$, I$^-$, AcO$^-$, BzO$^-$, HPO$_4^{2-}$, H$_2$PO$_4^-$, HSO$_4^-$, PF$_6^-$, BF$_4^-$, ClO$_4^-$, HS$^-$, N$_3^-$, HSO$_3^-$, CN$^-$ (Fig. S8 and S9, ESI†) as well as some neutral analytes such as phenylalanine (Phe), glutamic acid (Glu), alanine (Ala), glycine (Gly), lysine (Lys), leucine (Leu), proline (Pro), arginine (Arg), glutamine (Gln), valine (Val), histidine (His), methionine (Met), tryptophan (Trp), tyrosine (Tyr), cysteine (Cys), homocysteine (Hcy) and glutathione (GSH) (Fig. 3a and b). In the UV-vis study the λ_{max} (at 502 nm) got depleted only in the case of Cys with complete bleaching of the pink color similarly, in the emission spectrum, only Cys was able to cause a ratiometric change in the emission wavelength from 492 to 625 nm, whereas the other analytes including some of the foremost interfering analytes such as Hcy, GSH and NaHS were not able to cause any significant alteration (Fig. 3c). Thus our rational modification in the earlier reported probe BHI, not only lead to better detection limit and time response but also enhanced the selectivity of the modified probe **R1**.

Time response and pH study

We also monitored the time-dependent changes in the emission spectrum of **R1** upon the addition of 10 equivalents of Cys and the time response curve was plotted as intensity (at 492 and 625 nm) *versus* time (min.) (Fig. 4a). The same showed that the emission intensity reached to a plateau within 1.0 minute which is quite faster than the earlier reports (Table S1, ESI†). Further to explore the effect of pH on the sensing ability of the probe **R1**, we also checked its pH response in the absence and in the presence
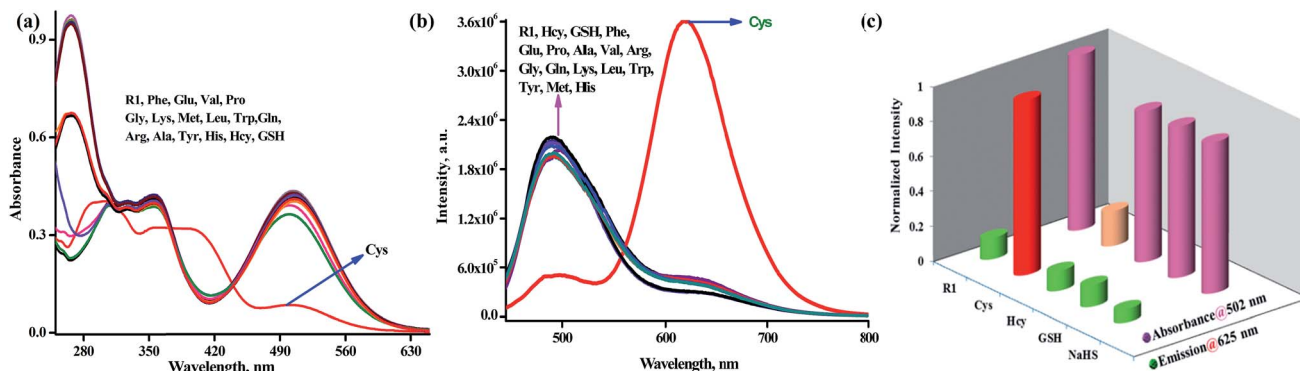

Fig. 2 (a) UV-visible titration spectrum of **R1** (10 μM) with Cys, (b) corresponding intensity plot and colorimetric response of **R1** with Cys (inset); (c) fluorescence titration spectrum of **R1** (1.0 μM) with Cys; (d) corresponding intensity plot and fluorescence response of **R1** with Cys (inset).

Fig. 3 (a) UV-vis and (b) fluorescence response of **R1** with different amino acids; (c) bar graph representation for the selectivity of **R1** towards thiols.
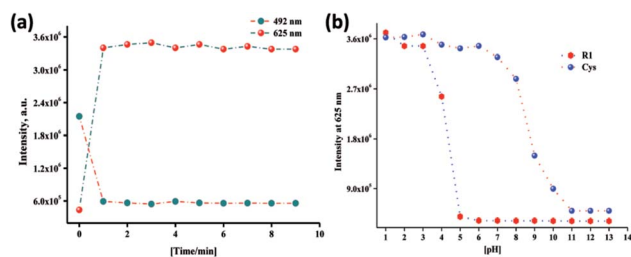
Fig. 4 (a) Reaction time profile of **R1** with Cys and (b) pH study of the **R1** in the absence and presence with Cys.

Fig. 6 HOMO–LUMO energy gap between **R1** and **R1**-Cys, showing weakening of ICT.

of the Cys. The pH graph plotted against the fluorescence intensity (Fig. 4b) showed that probe **R1** can be successfully utilized as sensor for the Cys in wide pH window from 5 to 9.

^{1}H NMR and HRMS study

For the detail mechanistic aspect of the above findings, we further compared the ^{1}H-NMR spectrum of **R1** with the isolated **R1**-Cys adduct (Fig. 5). The overlaid ^{1}H NMR spectrum showed that the aldehydic proton of **R1** at 9.67 ppm got disappeared in **R1**-Cys and a new peak at 5.76 ppm was appeared, which was assigned for the methine proton of the thiazolidine ring.[46–48] Other aromatic protons in **R1**-Cys however, got slightly up filled shifted in comparison to **R1**. Furthermore, to verify our proposed mechanism (Fig. S10, ESI†), the reaction product of **R1** with Cys was analyzed by high-resolution mass spectrometry analysis (HRMS), which displayed the formation of a **R1**-Cys adduct at $m/z = 532.08179$ (Fig. S11, ESI†).

Theoretical calculations

The optical response of **R1** indicated that the addition of Cys shifts the equilibrium towards the keto form. To explore the detailed possible mechanism we took help of the Density Functional Theory (DFT) with B3LYP/6-31 basis sets. The energy minimized structure of **R1** and **R1**-Cys has been presented in Fig. S12, ESI.†

In the enolic form, **R1** showed a very strong hydrogen bonding (1.69 Å) between the H of hydroxyl and N of benzothiazole which suggests the excited state intramolecular proton transfer (ESIPT) requirements.[49] On further comparing HOMO–LUMO gaps of **R1** and **R1**-Cys we found that the energy difference between the HOMO–LUMO in **R1**-Cys (3.11 eV) was quite larger than the **R1** (2.03 eV) (Fig. 6), confirming the weakening of ICT.
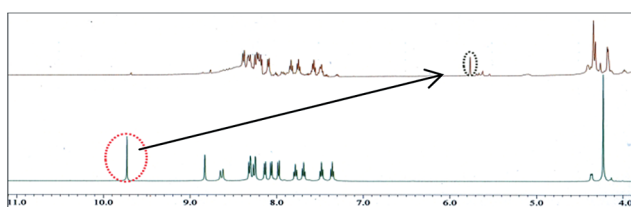
Sensing mechanism

The optical and theoretical studies of **R1** in the absence and in the presence of Cys along with a number of other analytes clearly indicate, that in the absence of the Cys, **R1** acted as strong ICT probe (with absorption maximum at 502 nm) having weak ESIPT emission at 492 nm (N*). As soon as there was nucleophilic attack of cysteine on the electrophilic carbonyl group, the ICT within the system got weakened and simultaneously the ESIPT underwent enhancement. Consequently the keto emission (T*, 625 nm) was observed in the red region. Thus simultaneously weakening of the ICT and strengthening of ESIPT enabled the selective colorimetric as well ratiometric fluorescent sensing of Cys possible (Fig. 7).

Cell imaging

The astonishing response of **R1** towards cysteine motivated us to check its applicability in the live cell imaging. In order to perform bioimaging of Cys in HeLa cells, initially a MTT assay was carried out to determine the viability of cells. After 24 hours treatment with **R1** (5 to 25 μM) this study showed that that the cell viability was about 90% when the concentration of **R1** was lower than 10 μM (Fig. S13, ESI†). Hence the probe **R1** was found to have very low toxicity to culture cells under the experimental conditions and was further use for cell imaging study.

The fluorescence microscopic imaging of **R1** (5 μM) into the HeLa cells were studied after a time lag of 24 hours. The necessary treatments were performed and images were taken in different channels (blue, green and red) to mark the ratiometric effect of **R1** in the presence of cysteine in the live cells. Fig. 8, showed that **R1** possesses good membrane permeability and is able to detect intracellular Cys in HeLa cells in the red channel.

Fig. 5 An overlay ^{1}H NMR spectrum of **R1** (below) and **R1**-Cys (above).
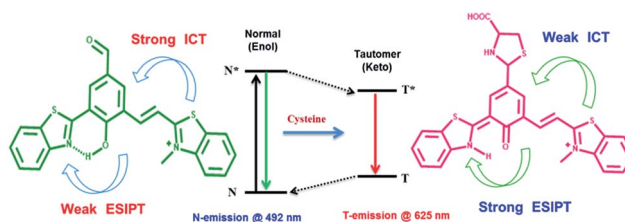

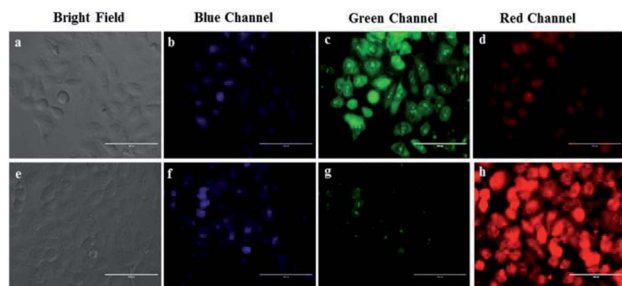Fig. 7 Proposed mechanism for the sensing of Cys through **R1**.

Fig. 8   Image of HeLa cell (a–d) bright and fluorescence image of R1; (e–h) bright and fluorescence image of R1 in presence of cysteine, in different channels.
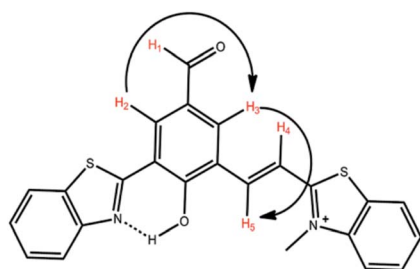

Fig. 9   Showing ^{1}H–^{1}H COSY correlations of R1.

Therefore, in comparison to the probes emitting in the visible region R1 has high potential for biological applications.

Experimental

Instrumentation and methods

The ^{1}H and ^{13}C NMR spectra were recorded on JEOL AL 500 FT NMR spectrometer in DMSO-d_6 while the Fourier transform infrared (FT-IR) spectra were obtained in the range of 4000–400 cm^{-1} using KBr pellets on a Perkin-Elmer spectrometer. Mass spectrometric analysis was carried out on a MDS Sciex API 2000 LCMS spectrometer. UV-visible spectra were obtained at room temperature (298 K) on a UV-1800 pharmaspec spectrophotometer with quartz cuvette (path length = 1 cm). The emission spectra were recorded on JY HORIBA fluorescence spectrophotometer at room temperature.

Synthesis of probe R1

R1 was synthesized by the simple condensation of BHI with benzothiazolium iodide in ethanol in the presence of small amount of base (20 μL of 0.5 M, NaOH). The reaction mixture was stirred for 8 hours, resulting into shiny dark color product which was filtered and finally washed with diethyl ether and dried in vacuum (Scheme 3). The isolated product was well characterized through various spectroscopic techniques (Fig. S14–S17, ESI†). Yield; 73%: IR (cm^{-1}): 3405, 3065, 2968, 2927, 1667, 1576, 1491, 1441, 1411, 1300, 1211, 1143; ^{1}H NMR (500 MHz, DMSO-d_6, TMS, ppm): 4.17 (3H, –CH$_3$), 7.30–7.32 (1H, –CH–), 7.41–7.43 (1H, –CH–), 7.44–8.77 (10H, –ArH), 9.67 (1H, –CHO), 13.33 (1H, –OH); ^{13}C NMR (125 MHz, DMSO-d_6,

TMS, ppm): 56.55, 109.35, 116.47–129.39, 136.28, 149.59, 152.03, 164.14, 173.5, 176.82, 189.49; HRMS: m/z calculated for $C_{26}H_{18}NS^+$ [M] = 429.07260, found = 429.07301. Along with the ^{1}H–^{1}H COSY NMR spectrum (Fig. S18, ESI†).

In the ^{1}H–^{1}H COSY spectrum (Fig. S18, ESI†), we found that the aromatic proton H3 and the olefinic proton H5 are coupled by each other (as shown in Fig. 9). While the aromatic proton H2 showed coupling only with aromatic proton H3, but not with the olefinic protons H4 or H5. Moreover, the absence of coupling of the olefinic proton H5 with the aromatic proton H2 further justifies the formation of *ortho*-adduct R1 (and not the *para*-adduct) by the condensation reaction.

Sample preparation for UV-visible and fluorescence studies

Due to partial solubility of the probe R1 in aqueous medium (at RT) the stock solution of the probe was prepared in DMSO at 1.0 × 10^{-3} M concentration. In this study above stock solution was further diluted to 1.0 × 10^{-5} M and 1.0 × 10^{-6} M for UV-vis and fluorescence studies respectively with H$_2$O and ACN in the ratio of 7 : 3 (v/v). The stock solutions (0.1 M) of the anions F$^-$, Cl$^-$, Br$^-$, I$^-$, AcO$^-$, BzO$^-$, HPO$_4{}^{2-}$, H$_2$PO$_4{}^-$, HSO$_4{}^-$, PF$_6{}^-$, BF$_4{}^-$, ClO$_4{}^-$, HS$^-$, N$_3{}^-$, HSO$_3{}^-$, as their sodium salts as well as neutral analytes such as phenylalanine (Phe), glutamic acid (Glu), alanine (Ala), glycine (Gly), lysine (Lys), leucine (Leu), proline (Pro), arginine (Arg), glutamine (Gln), valine (Val), histidine (His), methionine (Met), tryptophan (Trp), tyrosine (Tyr), cysteine (Cys), homocysteine (Hcy) and glutathione (GSH) were prepared in double distilled water and diluted to desired concentration further with double distilled water when needed.

Calculation of detection limits

The detection limit was determined using the IUPAC method. The S/N ratio was calculated from the absorption/emission intensity of sensor without any analyte (measured 10 times) and the standard deviations of blank measurements were determined. The detection limit was calculated as three times the standard deviation from the blank measurement divided by the slope of calibration plot between analyte concentration and fluorescence/absorption intensity of the receptor. The detection limit is then calculated with the following equation;[50]

$$\text{Detection limit} = 3Sd1/S$$

where, Sd1 is the standard deviation of blank measurement and S is the slope of the calibration curve.

Theoretical calculations

Theoretical calculations were performed with the Gaussian 03 program[51] based on the density functional theory (DFT) method. "Gauss View" was used for visualization of molecular orbital. Becke's three parameter hybrid functional with the Lee–Yang–Parr correlation functional (B3LYP) was employed for all the calculations.[52] The 6-31G** basis set was used to treat all atoms.[53]

Cell viability

MTT assay was done in order to check the viability of the cells. Eight thousand cells were seeded in 96-well plate and treated with different concentration of **R1** (5 to 25 μM). After 24 h of treatment, 10 μL MTT (3-(4,5-dimethylthiazol-2-yl)-2,5-diphenyltetrazolium bromide) solution (5 mg mL^{-1} in phosphate buffer) was added in each well. Subsequently, after 2 h of incubation at 37 °C, 100 μL DMSO was added to dissolve the formazan crystal and finally the absorbance was measured using an ELISA plate reader.

Methods for cell culture and bio-imaging

Stock solution of **R1** was made in DMSO with 100 mM concentration and further diluted in Dulbecco's Modified Eagle's Medium (DMEM). The small aliquot of DMSO solution of **R1** was completely soluble in water. The final concentration of DMSO was not exceeded from 0.1% during treatment of cells with compound. The fluorescent properties of **R1** into the HeLa cells were studied after a time lag of 24 hours. The necessary treatments were performed and images were taken in inverted fluorescent microscope (EVOS, Invitrogen) at concentration of **R1** (5 μM).

Conclusions

Thus, we successfully demonstrated a benzothiazole–benzothiazolium conjugate as a new HBT type probe (**R1**) which provides fine tuning of ICT and ESIPT. The systematic structural difference in **R1** and already reported probe BHI, made **R1** highly selective towards Cys over Hcy/GSH. Nevertheless, **R1** also acted as a highly sensitive probe for the colorimetric as well as ratiometric fluorescent sensing of Cys in the red channel with a fast time response in comparison to BHI. The ratiometric fluorescent change from green to red channel provided a wider possibility for biological applicability of **R1** as compared to many other previously reported probes for the same purpose based on HBT derived platform.

Acknowledgements

Notes and references

1 L. Y. Niu, Y. Z. Chen, H. R. Zheng, L. Z. Wu, C. H. Tung and Q. Z. Yang, *Chem. Soc. Rev.*, 2015, **44**, 6143–6160.

2 Y. Zhou, *Chem. Soc. Rev.*, 2012, **41**, 52–67.

3 W. Lin, L. Long, L. Yuan, Z. Cao, B. Chen and W. Tan, *Org. Lett.*, 2008, **10**, 5577–5580.

4 B. Liu, J. Wang, G. Zhang, R. Bai and Yi. Pang, *ACS Appl. Mater. Interfaces*, 2014, **6**, 4402–4407.

5 Y. Liu, D. Yu, S. Ding, Q. Xiao, J. Guo and G. Feng, *ACS Appl. Mater. Interfaces*, 2014, **6**, 17543–17550.

6 D. Brömme and S. Wilson, Role of Cysteine Cathepsins in Extracellular Proteolysis, in *Extracellular Matrix Degradation; Biology of Extracellular Matrix 2*, ed. W. C. Parks and R. Mecham, 2011, ch. 2, DOI: 10.1007/978-3-642-16861-1-2.

7 C. E. Paulsen and K. S. Carroll, *Chem. Rev.*, 2013, **113**, 4633–4679.

8 S. A. Lee, J. J. Lee, J. W. Shin, K. S. Min and C. Kim, *Dyes Pigm.*, 2015, **116**, 131–138.

9 Q. Han, Z. Shi, X. Tang, L. Yang, Z. Mou, J. Li, J. Shi, C. Chen, W. Liu, H. Yang and W. Liu, *Org. Biomol. Chem.*, 2014, **12**, 5023–5030.

10 J. A. Mc Mahn, T. J. Green, C. M. Skeaff, R. G. Knight, J. I. Mann and S. M. N. Williams, *Engl. J. Med.*, 2006, **354**, 2764–2772.

11 J. Deng, Q. Lu, Y. Hou, M. Liu, H. Li, Y. Zhang and S. Yao, *Anal. Chem.*, 2015, **87**, 2195–2203.

12 V. Kumar, A. Kumar, U. Diwan and K. K. Upadhyay, *Chem. Commun.*, 2012, **48**, 9540–9542.

13 T. W. Bell and N. M. Hext, *Chem. Soc. Rev.*, 2004, **33**, 589–598.

14 V. Kumar, A. Kumar, U. Diwan, M. K. Singh and K. K. Upadhyay, *Org. Biomol. Chem.*, 2015, **13**, 8822–8826.

15 L. M. Laglera, J. Downes, A. T. Sánchez and D. Monticelli, *Anal. Chim. Acta*, 2014, **836**, 24–33.

16 F. Zhang, J. Zhu, J. J. Li and J. W. Zhao, *Sens. Actuators, B*, 2015, **220**, 1279–1287.

17 U. Diwan, V. Kumar, R. K. Mishra, N. K. Rana, B. Koch, M. K. Singh and K. K. Upadhyay, *Anal. Chim. Acta*, 2016, **929**, 39–48.

18 Z. Song, R. T. K. Kwok, E. Zhao, Z. He, Y. Hong, J. W. Y. Lam, B. Liu and B. Z. Tang, *ACS Appl. Mater. Interfaces*, 2014, **6**, 17245–17254.

19 L. Yuan, W. Lin, B. Chen and Y. Xie, *Org. Lett.*, 2012, **14**, 432–435.

20 S. Xue, S. Ding, Q. Zhai, H. Zhang and G. Feng, *Biosens. Bioelectron.*, 2015, **68**, 316–321.

21 J. Zhang, J. Wang, J. Liu, L. Ning, X. Zhu, B. Yu, X. Liu, X. Yao and H. Zhang, *Anal. Chem.*, 2015, **87**, 4856–4863.

22 D. Zhang, M. Zhang, Z. Liu, M. Yu, F. Li, T. Yi and C. Huang, *Tetrahedron Lett.*, 2006, **47**, 7093–7096.

23 F. Kong, R. Liu, R. Chu, X. Wang, K. Xu and B. Tang, *Chem. Commun.*, 2013, **49**, 9176–9178.

24 X. F. Yang, Q. Huang, Y. Zhong, Z. Li, H. Li, M. Lowry, J. O. Escobedoc and R. M. Strongin, *Chem. Sci.*, 2014, **5**, 2177–2183.

25 Hi. Yao and T. Funada, *Chem. Commun.*, 2014, **50**, 2748–2750.

26 F. S. Santos, E. Ramasamy, V. Ramamurthy and F. S. Rodembusch, *J. Mater. Chem. C*, 2016, **4**, 2820–2827.

27 P. Majumdar and J. Zhao, *J. Phys. Chem. B*, 2015, **119**, 2384–2394.

28 J. Zhao, S. Ji, Y. Chen, H. Guo and P. Yang, *Phys. Chem. Chem. Phys.*, 2012, **14**, 8803–8817.

29 S. Barman, S. K. Mukhopadhyay, M. Gangopadhyay, S. Biswas, S. Dey and N. D. P. Singh, *J. Mater. Chem. B*, 2015, **3**, 3490–3497.

30 S. Park, O. H. Kwon, Y. S. Lee, D. J. Jang and S. Y. Park, *J. Phys. Chem. A*, 2007, **111**, 9649–9653.

31 T. Gao, P. Xu, M. Liu, A. Bi, P. Hu, B. Ye, W. Wang and W. Zeng, *Chem.–Asian J.*, 2015, **10**, 1142–1145.

32 S. W. Luo, H. Jiang, K. Zhang, W. Liu, X. Tang, W. Dou, Z. Ju, Z. Li and W. Liu, *J. Mater. Chem. B*, 2015, **3**, 3459–3464.

33 Y. Xu, L. Xiao, S. Sun, Z. Pei, Y. Peia and Y. Pang, *Chem. Commun.*, 2014, **50**, 7514–7516.

34 W. Sun, S. Li, R. Hu, Y. Qian, S. Wang and G. Yang, *J. Phys. Chem. A*, 2009, **113**, 5888–5895.

35 S. Goswami, A. Manna, S. Paul, A. K. Das, P. K. Nandi, A. K. Maity and P. Saha, *Tetrahedron Lett.*, 2014, **55**, 490–494.

36 X. Yang, Y. Guo and R. M. Strongin, *Angew. Chem., Int. Ed.*, 2011, **50**, 10690–10693.

37 Y. Kim, M. Choi, S. Seo, S. T. Manjare, S. Jonc and D. G. Churchill, *RSC Adv.*, 2014, **4**, 64183–64186.

38 X. F. Yang, Q. Huang, Y. Zhong, Z. Li, H. Li, M. Lowry, J. O. Escobedoc and R. M. Strongin, *Chem. Sci.*, 2014, **5**, 2177–2183.

39 X. Zhang and J. Y. Liu, *Dyes Pigm.*, 2016, **125**, 80–88.

40 F. Kong, R. Liu, R. Chu, X. Wang, K. Xu and B. Tang, *Chem. Commun.*, 2013, **49**, 9176–9178.

41 D. Maity and T. Govindaraju, *Org. Biomol. Chem.*, 2013, **11**, 2098–2104.

42 A. Marini, A. M. Losa, A. Biancardi and B. Mennucci, *J. Phys. Chem. B*, 2010, **114**, 17128–17135.

43 Z. Yuan, Q. Tang, K. Sreenath, J. T. Simmons, A. H. Younes, D. Jiang and L. Zhu, *Photochem. Photobiol.*, 2015, **91**, 586–598.

44 C. C. Hsieh, C. M. Jiang and P. T. Chou, *Acc. Chem. Res.*, 2010, **43**, 1364–1374.

45 J. Massue, G. Ulrich and R. Ziessel, *Eur. J. Org. Chem.*, 2013, **2013**, 5701–5709.

46 O. Rusin, N. N. S. Luce, R. A. Agbaria, J. O. Escobedo, S. Jiang, I. M. Warner, F. B. Dawan, K. Lian and R. M. Strongin, *J. Am. Chem. Soc.*, 2004, **126**, 438–439.

47 A. Poirel, A. D. Nicola and R. Ziessel, *J. Org. Chem.*, 2014, **79**, 11463–11472.

48 P. Das, A. K. Mandal, N. B. Chandar, M. Baidya, H. B. Bhatt, B. Ganguly, S. K. Ghosh and A. Das, *Chem.–Eur. J.*, 2012, **18**, 15382–15393.

49 S. Sahana, G. Mishra, S. Sivakumar and P. K. Bharadwaj, *Dalton Trans.*, 2015, **44**, 20139–20146.

50 B. Zhu, C. Gao, Y. Zhao, C. Liu, Y. Li, Q. Wei, Z. Ma, B. Du and X. Zhang, *Chem. Commun.*, 2011, **47**, 8656–8658.

51 M. J. Frisch, *et al.*, *GAUSSIAN 03, (Revision D.01)*, Gaussian, Inc., Wallingford, CT, 2004.

52 D. A. Becke, *J. Chem. Phys.*, 1993, **98**, 5648–5652.

53 C. Lee, W. Yang and R. G. Parr, *Phys. Rev. B: Condens. Matter Mater. Phys.*, 1988, **37**, 785–789.